MMA Memo 214: Hybrid arrays: the design of reconfigurable aperture-synthesis interferometers

Adrian Webster
Royal Observatory Edinburgh, Scotland

June 4, 1998

Abstract

Modern aperture-synthesis array telescopes usually have several configurations differing in size in order to provide the observer with a selection of compromises between angular resolving power and sensitivity. The layout of each configuration, however, is a choice for the designer of the telescope, the main consideration being the desired taper in the uv-plane coverage, which determines such properties as the sidelobe level, the width of the synthesised beam and the relative sensitivity to compact and extended components of the source. There is, unfortunately, no simple way of making this latter choice because it can depend on the source under study and on the particular reasons for making the observations. Implementing two or more types of configuration at each size would solve the problem but the cost of additional antenna stations usually rules this out, while weighting the baselines to change the taper in software reduces the sensitivity. It is therefore investigated to what extent an array may be converted from one type to another by removing some of the dishes from one configuration and resiting them on existing stations of the next smaller configuration to yield a hybrid array. Telescopes are considered whose basic configurations are concentric rings consisting either of circles or of Reuleaux triangles, both of which have a low ratio of the numbers of short baselines to long; moving some of the dishes to a smaller configuration then increases the ratio by providing additional short and medium baselines. Some of the hybrid arrays generated in this way are found to have reasonable radial profiles in the uv-plane providing the multiplicative scale factor between successive configurations is not too large, no more than about 3 or 4. Reuleaux triangles are found to be superior to circles for hybrid arrays not only because their radial profiles are smoother at all values of the scale factor but also because their desirable properties degrade more slowly as the scale factor is increased.

1 Introduction

When the number of antennas in a new aperture synthesis array and the highest desired angular resolution are settled, there are still many decisions to be made in designing the layout of the stations for the antennas. Minimizing the cost is an important factor, which generally requires keeping the number of stations to a minimum and arranging the stations in a way that reduces the length of roadway, cabling and other services required to link them to the central laboratory. One of the direct consequences is that it is usually feasible to build only a small number of configurations of different size, and, although it would be desirable from the astronomer's point of view to have a series of many configurations, with successive members differing from each other in scale by only by a modest factor so that it would be easy to select one that is well matched to any particular astronomical source, the cost of the large number of stations required would be prohibitive. It follows that, in order to provide a wide range of beamwidths, the configurations inevitably differ in size by a relatively large multiplicative scaling factor; for the MMA this scale factor seems likely to be of order 4 (Holdaway 1998).

There is another important consideration that is affected by a similar compromise between flexibility and the cost of stations, namely the choice of the geometrical layout for each configuration. The issue here is that, for any required angular resolution, it is possible to design layouts with different forms for the taper (i.e. the dependence of the density of baselines in the uv-plane as a function of baseline length), but there is no ideal or optimal choice between these alternatives. There are two major types of layout: those that give a relatively uniform coverage of the uv-plane and have a small value for the ratio of the number of short baselines to the number of long, and those that give a centrally-condensed distribution in the uv-plane and have a large value for the ratio. Both types have their uses, and which is the better choice for a particular observation depends not only on the source but also on the reason for observing it. Compact, simple sources lacking large scale structure may be better observed with the first type of configuration, because the many long baselines give a sharp image and the relatively small number of short baselines is unimportant when there is little large-scale structure to be measured, but complex sources with structure on a wide range of angular scales may be better observed with the second type. The purpose of the observation also enters: if the attention is on the compact components of a complex source, perhaps for photometry or astrometry or to discover whether they can be resolved further into subcomponents, the first type is likely to be preferable, whereas if it is required to produce a map of the same source that provides a good representation of components of all sizes, or one that lacks strong sidelobes on the main beam, the second type is the more natural choice. A telescope with two or more configurations available at each size would be ideal because the astronomer could then choose one with a taper appropriate to the purpose, but the cost of the extra stations usually rules this out and it is necessary to select one type at the design stage of the project and to build the telescope accordingly. The choice is not straightforward, and there is a debate in progress about which type would be better for the MMA (Holdaway 1998).

We do not wish to enter this debate here, but prefer to consider instead whether it is possible to circumvent the issue entirely by designing an array that is reconfigurable between the two types while costing no more than either type alone. In a sense, a solution of this kind already exists because the taper can be altered in software when deriving the maps by applying weights to the baselines that depend systematically on the baseline length, but a large change in taper is unavoidably associated with a large degradation of the sensitivity of the telescope, and a different approach is investigated here that does not suffer from this difficulty. The idea is that, even when only one type of configuration is available there will be several copies of that configuration differing in size, and it is then possible to consider distributing the antennas over more than one of them to yield a hybrid configuration. If this can be done in such a way as to provide an array with a taper that is not only different but also useful, a more flexible instrument would result and the astronomer could select whichever configuration seems more appropriate for the project in hand. There would, moreover, be little impact on the construction cost because no additional stations need be built.

It is not obvious from the outset whether this strategy is likely to be successful, because the siting of the stations needed to provide reconfigurability need not be consistent with that required merely to provide one particular configuration in several different sizes, and one of the principal aims of this study is to find out to what extent a design is feasible that can be reconfigured in a useful way. A second aim is to discover whether any restriction on the scale factor between consecutive sizes of configuration has to be imposed, and a third is to find out whether some types of basic configuration are more suited to reconfiguration than others.

2 Theory

The discussion so far has been general, no decision having been made about either the geometry of the basic configurations or where the configuations are sited relative to one another, and it is necessary to restrict the range of possibilities to a manageable level. It is therefore supposed that all the basic configurations are of identical shape and differ only in size. It is also decided that the largest configuration is to be reconfigurable, from which it immediately follows that the antennas that are redeployed out of this configuration are placed on the stations of smaller configurations. Another decision is that only the stations of the next smaller configuration are to be used in this way; the discussion is then applicable to the reconfiguration of all but the smallest configuration.

The nomenclature adopted is that the larger of the two configurations under discussion is referred to as A and the smaller as B, and their diameters (i.e. their longest internal baselines) are a and b respectively; the scale factor between configurations is then

$$s = a/b. \tag{1}$$

The baselines of the hybrid may be partitioned into three classes: AA, in which both antennas are sited on stations of configuration A; BB, with both on configuration B; and AB, with one on each configuration.

The antennas are taken to be sited on level ground, and for simplicity only snapshot mode is considered, so the coverage of the uv-plane consists of a collection of points rather than elliptical arcs. It is useful to define polar coordinates (w, θ) in the uv-plane with the radial coordinate normalised to the range $0 \leq w \leq 1$

$$w = \sqrt{u^2 + v^2}/a. \tag{2}$$

Another decision is to consider only concentric configurations, the centroid of the stations of configuration A being taken to coincide with the centroid of those of B. This is not an arbitrary decision but is required for isotropy: if the configurations are not concentric then the length of the baselines of class AB will depend systematically on orientation, which is undesirable because the synthesised beam should be as nearly circular as possible.

Another important matter is the layout of the basic configuration, which could be chosen either to have a centrally-condensed taper, with the aim of designing a hybrid with a uniform taper, or to have a uniform taper and the hybrid a centrally-condensed one. This is not in fact an open issue at this stage but has already been settled by the decision to resite the antennas taken from A only on the stations of a smaller configuration B when constructing the hybrid, because antenna pairs of class BB will provide additional short baselines and those of class AB will provide additional medium baselines, but there will be fewer long baselines as a result of the depletion of baselines of type AA. Such a change in the relative abundance of baselines as a function of length would be inappropriate for a basic configuration that is already well endowed with short and medium baselines, so the basic configuration is taken to have a uniform taper that may be converted to a more centrally-condensed one by hybridisation. Rings are therefore adopted for the basic configurations, and hybrid arrays based on the two most commonly-discussed types of ring, namely circles and Reuleaux triangles, are now considered.

2.1 Radial profiles in the uv-plane

In order to investigate the properties of hybrid circular arrays it is simplest to adopt a continuum model, equivalent to siting an infinite number of dishes uniformly on the circumference, and to consider the function $p(w)$, where $p(w)\mathrm{d}w$ is the fraction of baselines with length between w and $w + \mathrm{d}w$. For baselines of class AA this is

$$p_{\mathrm{AA}} = \frac{2}{\pi\sqrt{1 - w^2}}, \tag{3}$$

for class BB

$$p_{\mathrm{BB}} = \begin{cases} \dfrac{2s}{\pi\sqrt{1 - s^2 w^2}} & \text{for } w \le 1/s \\ \\ 0 & \text{otherwise,} \end{cases} \tag{4}$$

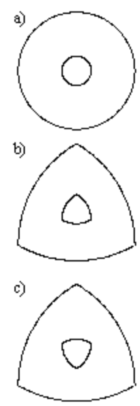

Figure 1: The three layouts considered in the text. a) Circles. b) Symmetrical Reuleaux triangles. c) Antisymmetrical Reuleaux triangles. All three cases are drawn for a scale factor $s = 4$.

and for class AB

$$p_{\rm AB} = \begin{cases} \dfrac{8\,s^2\,w}{\pi\sqrt{4\,s^2 - (1 + s^2 - 4\,s^2\,w^2)^2}} & \text{for } (s-1)/2s \le w \le (s+1)/2s \\ \\ 0 & \text{otherwise.} \end{cases} \tag{5}$$

These curves are plotted in the top panel of Fig. 2 for the case $s = 4$.

Reuleaux triangles are based on three points sited at the vertices of an equilateral triangle, the 'side' joining any two vertices being a circular arc centred on the third vertex. They are harder to treat analytically, and the calculation is based instead upon a large but finite number of dishes (180) sited uniformly on the circumference of two nested Reuleaux triangles, 90 on each, the function p being estimated as a histogram of the large number of baselines formed by all possible pairs of each class; the scale factor is again taken to be $s = 4$. Nested Reuleaux triangles are not completely specified until the relative orientation of the two triangles is given and so the two configurations drawn in Fig. 1 are considered, giving two histograms for baselines of class AB (Fig. 2).

The radial profile of a hybrid array is a sum of the three curves from the different classes, the relative proportions depending on a single parameter which may be taken as f, the fraction of the antennas sited on configuration B. The composite profile is then approximately

$$p = (1-f)^2 p_{\rm AA} + 2f(1-f)p_{\rm AB} + f^2 p_{\rm BB}. \tag{6}$$

Whatever the value of f adopted, the resulting composite curve should ideally be smooth, resembling perhaps the curves given in Fig. 4 for two standard theoretical forms for centrally-condensed distributions in the uv-plane: a circular Gaussian density truncated at the 10 dB radius,

$$p = 5.117w\exp(-2.303w^2) \tag{7}$$

and that corresponding to a uniformly-filled aperture

$$p = \frac{16w}{\pi}\left[\cos^{-1}w - w\sqrt{1-w^2}\right]. \tag{8}$$

The smoothness of the composite curve is determined by several factors, two of which are particularly important, namely the continuity of the curves

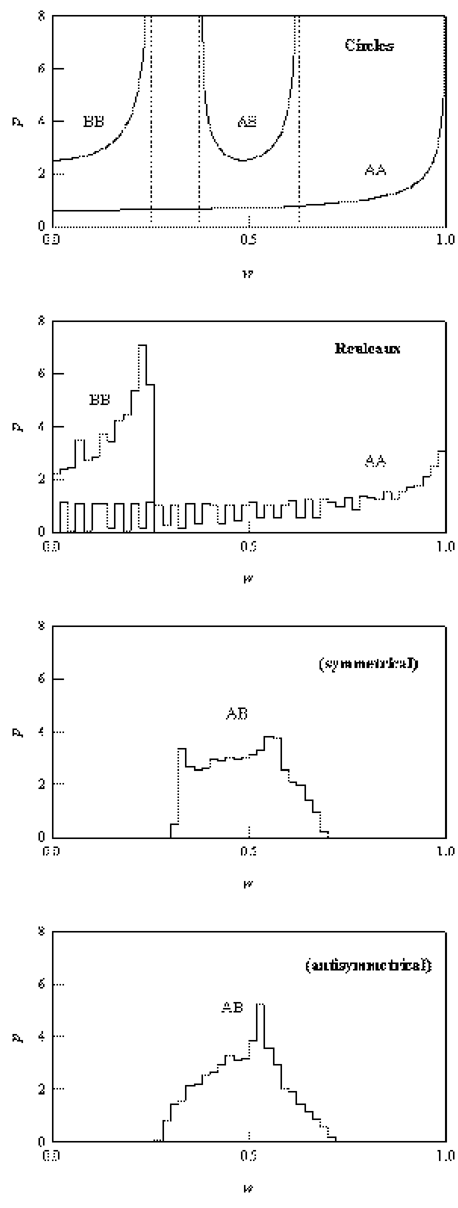

Figure 2: Contributions to the radial profiles, for scale factor $s = 4$. Top: concentric circles. Remainder: Reuleaux triangles.

Table 1: The critical scale factor for different types of configuration.

Configuration	s_c
Circles	3.00
Symmetrical Reuleaux	3.37
Antisymmetrical Reuleaux	3.73

from different classes of baseline and the smoothness of those curves individually. The different classes of baseline are defined over different ranges of the independent variable w, and it is quite possible for there to be a discontinuity in the form of a gap between the ranges of classes BB and AB, as may be seen in all three cases in Fig. 2. Such a gap is undesirable because it prevents the curves for BB and AB being joined smoothly, whatever the value of f. A gap is only present when $s > s_c$, where s_c is a critical value that depends on the type of configuration under study (Table 1). The value of s_c associated with a configuration is, in a sense, a figure of merit for that configuration; one of the desirable properties of a hybrid array is that it should produce reasonable radial profiles even at large values of s, and so a large value of s_c is better than a small one. It may be seen from Table 1 that Reuleaux hybrids have better figures of merit than circular ones, and that the antisymmetrical type of Reuleaux hybrid has a better figure than the symmetrical. The values of s_c are such that it may be possible to design a hybrid array with a smooth radial profile for values of s as large as $3 - 4$, but not much larger.

The smoothness of the individual curves is the second important factor. The curves for circles all have singularities, which arise at values of w close to the minimum and maximum for the configurations involved. The symmetry of the circular arrays is so high that the distribution of baselines lengths involving any one antenna is the same whichever antenna in a particular configuration is chosen, and as a result the distributions superpose to give the marked singularities in the curves seen in Fig. 2. The curves p_{AA} and p_{BB} have one singularity each, at the greatest value of w for each class, while p_{AB} has two, one at each end of the range. These singularities are formal in nature, arising as a result of the decision to investigate a model that consists effectively of an infinite number of infinitessimal dishes, but in practice a circular interferometer with a finite number of dishes would have finite peaks at the same values of w which would be just as undesirable.

The curves for the Reuleaux triangles are smoother, because although the lengths of the baselines for any particular dish on the inner triangle have stationary values at some point on each of the three sides of the outer triangle, the baseline lengths at which they occur are not in general the same for all the dishes on the inner triangle and the superposed curves are smoother than for circles. The sole exception is for dishes near the mid-points of the sides of the inner triangles, whose baselines show stationary values at similar baseline lengths for one particular side of the outer triangle (the adjacent side for the symmetrical case and the opposite side for the antisymmetrical) and these give rise to weak peaks in $p_{\rm AB}$ at $w = 0.33$ and 0.53 respectively, as seen in Fig. 2.

There also exist opportunities for joining the Reuleaux curves smoothly: the height of the left-hand extremity of $p_{\rm AB}$ for the symmetrical case may, for an appropriately-chosen value of f, be made to match that of the right-hand extremity of $p_{\rm BB}$, yielding a smooth join. A smooth join may also be achieved for the antisymmetrical case, particularly for values of s that allow a little overlap between these curves. Furthermore, both curves of type $p_{\rm AB}$ for Reuleaux triangles decline smoothly to zero for large θ (i.e. $0.55 < \theta < 0.75$), enabling a smooth transition to $p_{\rm AA}$ in the composite profile. It is therefore to be expected on these general grounds that it should be possible to generate smoother radial profiles for Reuleaux triangles than for circles.

2.2 Beam profiles

In order to see how these theoretical ideas might translate into practice, the beam profiles were calculated for interferometers with a finite number of dishes. The number of dishes was taken as 60, a value typical of designs for the next generation of millimetre arrays, and a value of $f = 0.4$ chosen as giving some degree of match between $p_{\rm BB}$ and $p_{\rm AB}$, so 36 of the dishes were sited uniformly on configuration A and 24 similarly on configuration B. The distribution of the baselines in the uv-plane lacks circular symmetry and it is to be expected that the resulting beam profiles also lack it. For the purpose of this initial investigation the variation of the radial beam profiles with position angle about the beam centre is a secondary complication that may be set aside by calculating the average beam profile $\Psi(\theta)$ as the Hankel transform of $\sigma(w)$, the surface density of points in the uv-plane, as though it has circular symmetry (e.g. Bracewell 1965),

$$\sigma(w) = \frac{p(w)}{2\pi w} \tag{9}$$

giving

$$\Psi(\theta) = 2\pi \int_0^\infty \sigma(w) \mathrm{J}_0\,(2\pi w\theta)\, w \mathrm{d}w \tag{10}$$

$$= \int_0^1 p(w) \mathrm{J}_0\,(2\pi w\theta)\, \mathrm{d}w \tag{11}$$

where λ is the observing wavelength, J_0 is the Bessel function and θ is the angle from the beam centre measured in units of λ/a radians. The normalization of $p(w)$ adopted throughout this paper is

$$\int_0^1 p(w)\mathrm{d}w = 1 \tag{12}$$

and so it follows that the beam profile is normalized to a forward gain of unity: $\Psi(0) = 1$.

Beam profiles are given in Fig. 3 for hybrid arrays of circles and symmetrical Reuleaux triangles, for s=2, 3, 4 and 5, where it may be seen that the sidelobe levels for the circles are, on the whole, higher than those for the corresponding Reuleaux triangles. For the circles, the hybrid with $s = 2$ has the best properties. It lacks a strong peak near $\theta = 2.2$, where most of the curves have their first sidelobe, and instead has its strongest peak near $\theta = 4.5$, and that peak is a relatively weak one with $\Psi = 0.048$; at greater values of θ the remaining lobes are agreeably weak. The other curves for circles are poorer, particularly those for realistic values of the scale factor ($s \approx 4$); they have strong first lobes ($\Psi(2.15) = 0.099$ for $s = 4$) and do not decline particularly rapidly thereafter. The curves for the Reuleaux hybrids are systematically better, and while the beam for $s = 4$ still has a relatively strong first lobe ($\Psi(2.2) = 0.081$), that lobe is weaker than the corresponding lobe for the circles. The amplitude of the beam pattern also declines faster to low values beyond the first lobe.

A comparison between the two types of Reuleaux triangle is presented in Fig. 4 for the case $f = 0.4, s = 4$, and the radial profiles in the uv-plane are also given. The beam profiles are similar and there is little to choose between them in terms of quality: the first lobe of the antisymmetrical hybrid is marginally the stronger ($\Psi = 0.085$ as against 0.081) but at larger θ

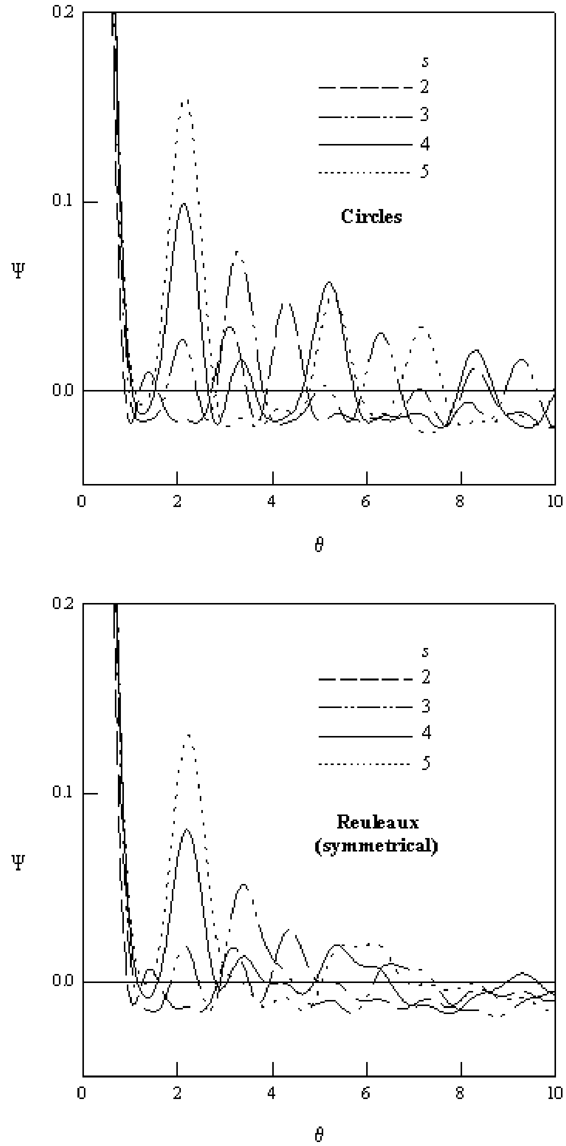

Figure 3: Beam profiles averaged over position angle, for f=0.4 and the values of s given in the key. Above: circles. Below: symmetrical Reuleaux triangles.

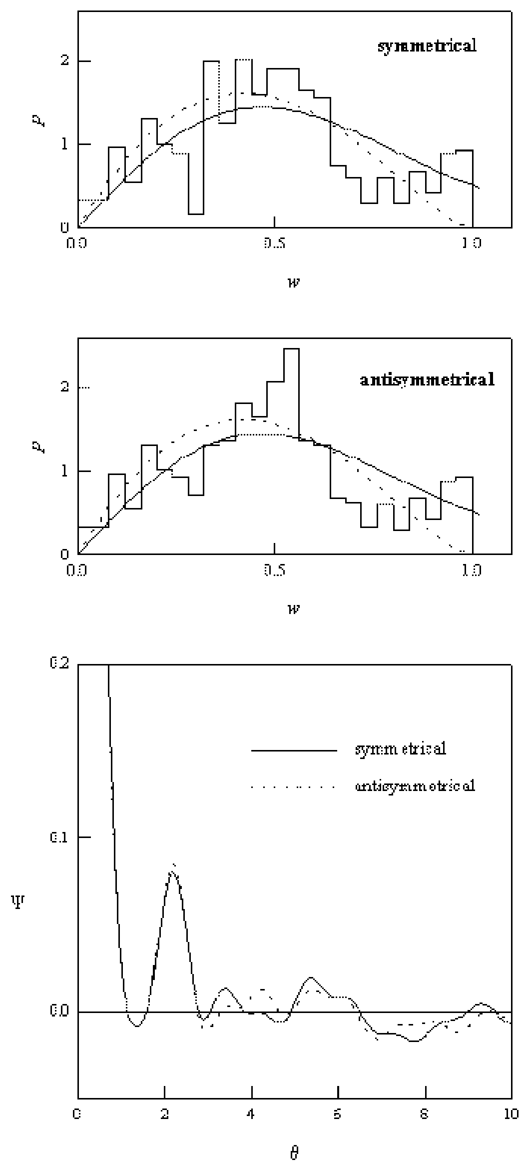

Figure 4: Radial profiles in the uv-plane and beam profiles for the two types of Reuleaux hybrid considered in the text. s=4 and f=0.4.

the root-mean-square amplitude is marginally the weaker (0.0079 as against 0.0094 for $3 \leq \theta \leq 10$).

As may be expected from the increased proportion of short and medium baselines, the Realeaux hybrids have synthesised beams broader than that of the simple Reuleaux configuration A from which they are derived. They are not much broader, however: the beams of both types of Reuleaux hybrid with $s = 4$, $f = 0.4$ (Fig. 4) are virtually identical, and have full widths to half maximum 1.29 times that of configuration A. This ratio is much smaller than the factor $s = 4$ for the ratio of beamwidths of the simple configurations B and A, and the hybridization of A has made relatively little difference to the beamwidth for these particular parameters.

3 Discussion and conclusions

The investigations of the radial profiles in the uv-plane and the synthesised beam shapes both point to the conclusion that the hybrids based on Reuleaux triangles are superior to those based on circles for realistic values of the scale factor s. Indeed, the hybrids based on circles have properties so poor that they seem unlikely to be of much use in practice.

The hybrids based on Reuleaux triangles have better properties, particularly the low level of sidelobes beyond the first, but the first lobe is still fairly strong for realistic values of s and the designs considered above might not be regarded as desirable for many purposes. The 10 dB Gaussian and the uniform distribution of antennas within a disk (Fig. 4) may be taken as paradigms for arrays with relatively large numbers of short and medium baselines, and they have first sidelobe levels of 0.014 and 0.017 respectively. The amplitudes of the first sidelobes of the Reuleaux hybrids with $s = 4$ and $f = 0.4$ are of order 0.08 and are therefore significantly greater, and although they are considerably weaker than the corresponding 0.13 of a single Reuleaux configuration, much depends on whether they can be reduced further. The properties are nevertheless remarkably good in view of the tightness of the constraints from the decision to use only the stations of existing configurations; if funding were available for 40% more stations to be sited at will with the aim of transforming the beam profile of a simple Reuleaux array into one with very low sidelobe levels, it is unlikely that one would choose to site them all near the centroid of the existing array, to site them on another Reuleaux configuration, or to site them in a region with an area less than 10 percent of that of the initial array.

There appear to be two general strategies that might be followed with the aim of improving the properties further: fine-tuning and fine-weighting. By fine-tuning is meant changing the details of the array geometry, such as the parameters s and f. In this preliminary study we have only investigated models on a coarse grid of s and for one value of f, and a more extensive calculation of the beam profiles on a fine grid of values for both parameters would be needed in order to assess how much improvement of this kind is possible. Another matter that might be fine-tuned is the distribution of the antennas on the stations of the basic configurations, which cannot in any case take the uniform distribution that was adopted here for simplicity, and it may be possible to use this degree of freedom constructively in order to improve the beam profile.

The beam profile may also be modified by weighting the measured complex correlation coefficients in software before the Fourier transform is applied, with an appropriately-chosen weight for each baseline. Weighting the baselines was discussed in the Introduction and rejected as a means of changing the effective beamwidth of an array because it reduces the sensitivity by too large a factor, but these considerations do not apply to the present case because the beamwidth of the hybrid is entirely acceptable. Gross weighting to change the beamwidth by a large factor is not required, merely fine weighting to smooth out the relatively minor irregularities in the uv-plane distribution. That can be done with weights that have a small dispersion about the mean, leading in consequence to a much lower reduction in the sensitivity. Such a technique could be employed not only to control the radial profile of the beam but also to reduce the variation of the profile with position angle about the beam centre.

Overall, this preliminary investigation is inconclusive. The best of the hybrid arrangements studied here have properties that are not quite good enough for use, but the possibilities for further improvement are not yet exhausted.

References

Bracewell R., 1965, The Fourier Transform and its Applications, McGraw-Hill, London

Holdaway M., 1998, MMA Configuration Design Concepts, http:/www.tuc.nrao.edu/mma/config/config.html